Doping Effects of Magnetic Impurities on the Spin-Peierls (*p*-CyDOV) and Dimer (*p*-BrDOV) Systems

Kazuo Mukai,*,† Yasuo Shimobe,† Javad B. Jamali,‡ and Norio Achiwa‡

Department of Chemistry, Faculty of Science, Ehime University, Bunkyo-cho, Matsuyama 790-8577, Japan, and Department of Physics, Faculty of Science, Kyushu University, Hakozaki, Fukuoka 812-0053, Japan

Received: March 30, 1999; In Final Form: October 4, 1999

The magnetic susceptibilities of the mixed radical crystals, $(p\text{-CyDOV})_{1-x}(p\text{-BrDOV})_x$ ($x = 0-1$), were measured to study the doping effect of magnetic impurities on the spin-Peierls (SP) transition of *p*-CyDOV (3-(4-cyanophenyl)-1,5-dimethyl-6-oxoverdazyl) and on the dimer state of *p*-BrDOV (3-(4-bromophenyl)-1,5-dimethyl-6-oxoverdazyl) radical crystals. *p*-BrDOV and *p*-CyDOV, which have van der Waals radii and unpaired spin distributions similar to each other and $S = {}^1/_2$ spin, were chosen as dopants in the above SP and dimer systems, respectively. The effect of doping on the SP system is very remarkable. The SP transition temperature ($T_{SP} = 15.0$ K) decreases rapidly upon *p*-BrDOV doping and the SP state almost disappears in the lightly doped sample with $x = 0.05$, although the effect of *p*-BrDOV doping was not observed in the powder X-ray diffraction pattern and the ESR spectrum of *p*-CyDOV at the low concentration region ($x = 0-0.09$) of *p*-BrDOV. The susceptibilities of mixed crystals with $x = 0.05$ and 0.07 can be well explained by the sum of the susceptibilities of one-dimensional (1D) Heisenberg antiferromagnet (χ_{1D-HAF}) with intrachain exchange interaction ($2J/k_B$) similar to that of pure *p*-CyDOV and Curie impurity (χ_{Curie}). Similarly, the temperature dependence of the susceptibilities for the mixed crystals with $x = 0.01$ and 0.03 above T_{SP} is described by the above two contributions (χ_{1D-HAF} and χ_{Curie}). However, the susceptibilities below T_{SP} can be explained by considering the contribution from the SP state (χ_{SP}) in addition to the above two contributions. On the other hand, the dimer state in *p*-BrDOV survives in the heavily doped sample with $x = 0.85$. The intradimer exchange interaction $2J/k_B$ remains constant between $x = 0.85$ and 1, suggesting that the substituted *p*-CyDOV molecules play a role as *p*-BrDOV ones in the mixed crystals with $x = 0.85-1$. This work is the first report of the effects of magnetic impurities on the organic SP transition system.

Introduction

The study of magnetic materials based on organic radical molecules has attracted considerable attention in recent years.[1] 6-Oxo- and -thioxoverdazyl radicals are well-known as one of the representative stable free radicals that can be isolated as solvent-free pure radicals in the crystalline state.[2,3] The magnetic properties of these radical crystals have been studied recently, and several interesting magnetic properties such as ferromagnetism,[4−7] weak ferromagnetism,[8−11] and spin-Peierls transition[12−14] have been observed.

In a previous work, we measured the magnetic susceptibility (χ_M) of the 3-(4-cyanophenyl)-1,5-dimethyl-6-oxoverdazyl (*p*-CyDOV) (Figure 1) radical crystal and found that the susceptibility (χ_M) of the *p*-CyDOV exhibits the characteristic properties of the spin-Peierls (SP) transition.[12] The χ_M of *p*-CyDOV shows a broad maximum at 54 K and decreases abruptly at SP transition temperature $T_{SP} = 15.0$ K. High-field magnetization data ($H = 0-35$ T) that provide clear evidence for a SP transition were reported. To our knowledge, this is the first example of a SP transition compound found for a genuine organic nonionic radical crystal.

The SP transition is well-known as one of the most interesting magnetic behaviors observed for organic radical salts, such as TTF−CuBDT and MEM−$(TCNQ)_2$.[15−17] The SP transition occurs when a system of uniform antiferromagnetic (AFM) Heisenberg linear chains undergoes a transformation to a system of dimerized or alternating AFM linear chains. This dimerization is mainly caused by the spin−phonon coupling between the one-dimensional (1D) spin system and the three-dimensional (3D) phonon system. The SP transition was also observed for the inorganic compound $CuGeO_3$.[18,19] However, the examples of SP transition compounds reported are very limited; there are only six including *p*-CyDOV as far as we know.

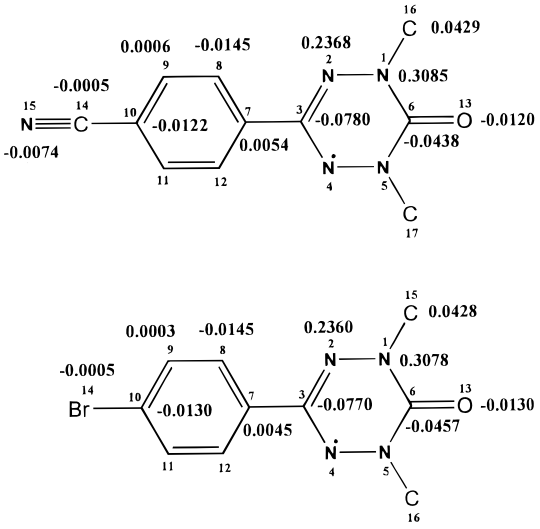

Figure 1. Molecular structures of *p*-CyDOV and *p*-BrDOV radicals, showing the numbering system and McLachlan unpaired spin densities.

The first report of the effect of impurities on the SP system

* To whom correspondence should be addressed. Fax: 81-89-927-9590. E-mail: mukai@sci.ehime-u.ac.jp.
† Ehime University.
‡ Kyushu University.

10.1021/jp991086p CCC: $18.00
Published on Web 11/19/1999

was performed for the $CuGeO_3$ system ($T_{SP} = 14.2$ K) by Hase et al.[19] In the $Cu_{1-x}Zn_xGeO_3$ system, the value of the SP transition temperature (T_{SP}) decreases rapidly with doping up to $x = 0.02$, and an AFM phase transition appears in the samples with $0.02 \leq x \leq 0.08$ below 5 K.[20,21] It is thought that the reduction of T_{SP} is due to disorder in AFM chains and that the disruption of the SP order leads to the occurrence of the AFM transition. The effect of nonmagnetic impurities, *p*-CyDOV−H (amine precursor of *p*-CyDOV), on the SP transition of the *p*-CyDOV crystal has also been studied recently, showing that the transition temperature reduced rapidly upon *p*-CyDOV−H substitution and the SP state disappeared around $x = 0.07$.[13] However, the occurrence of the AFM transition was not observed for the diluted *p*-CyDOV radical crystals, $(p\text{-CyDOV})_{1-x}(p\text{-CyDOV-H})_x$ above 4.2 K.

On the other hand, the magnetic susceptibility (χ_M) of the 3-(4-bromophenyl)-1,5-dimethyl-6-oxoverdazyl (*p*-BrDOV) (Figure 1) radical crystal can be well explained by the singlet−triplet equilibrium model (the dimer system) with the negative exchange interaction of $2J/k_B = -55$ K.

In the present work, the magnetic susceptibilities of 11 kinds of mixed radical crystals, $(p\text{-CyDOV})_{1-x}(p\text{-BrDOV})_x$ ($x = 0-1$), were measured to study the effects of magnetic impurities on the SP transition of *p*-CyDOV and on the dimer state of *p*-BrDOV. The powder X-ray diffraction patterns of the mixed radical crystals were measured to obtain the information on the crystal structure of the mixed radical crystals. The ESR measurements were also performed for these radical crystals. The McLachlan MO calculations[22] were performed for *p*-CyDOV and *p*-BrDOV radicals, to ascertain whether *p*-BrDOV has a spin density distribution similar to that of *p*-CyDOV or not. The present work provides the first example of the effect of magnetic impurities on the SP transition of organic compound.

Experimental Section

p-CyDOV and *p*-BrDOV were prepared according to the method of Neugebauer et al.[2] The powder samples of mixed radical crystals, $(p\text{-CyDOV})_{1-x}(p\text{-BrDOV})_x$ ($x = 0.01$, 0.03, 0.05, 0.07, 0.09, 0.26, 0.45, 0.65, 0.80, 0.85, 0.90, and 0.95), were obtained by the following procedures: The *p*-CyDOV and *p*-BrDOV crystals were dissolved into CH_2Cl_2 in the round-bottomed flask in the ratio of $1 - x$ to x at 20 °C. The CH_2Cl_2 solvent was slowly evaporated using a rotary evaporator. This flask was connected to a vacuum line (5×10^{-3} Torr) for 2 h to remove the CH_2Cl_2 solvent completely.

The paramagnetic susceptibility was measured in the temperature range 4.2−300 K by a SQUID magnetometer. Measurement was performed in the magnetic field H of 200 G to avoid saturation effects. The susceptibilities of the *p*-CyDOV and *p*-BrDOV radicals have been corrected for the diamagnetic contributions of $\chi_{dia} = -0.113 \times 10^{-3}$ and -0.138×10^{-3} emu/mol calculated by Pascal's method, respectively.

Powder X-ray diffraction patterns of the mixed radical crystals were measured by using a convergent monochromatic Cu Kα beam of the STOE transmission X-ray diffractometer with a curved germanium monochromator. During the measurement the samples were rotated in order to prevent a preferred orientation.

ESR measurements were carried out using a JES-FE-2XG spectrometer equipped with a Takeda-Riken microwave frequency counter.

Results

Magnetic Susceptibilities of *p*-CyDOV and *p*-BrDOV Radical Crystals. The magnetic susceptibility (χ_M) of the *p*-CyDOV radical crystal is shown in Figure 2a. The susceptibility above 15.0 K can be well described by the 1D Heisenberg linear chain model[23] with an AFM exchange interaction of $2J/k_B = -84$ K between neighboring spins, as reported in a previous work.[12] The χ_M of *p*-CyDOV decreases abruptly at the SP transition temperature $T_{sp} = 15.0$ K. The residual paramagnetic radical concentration, calculated from the susceptibility at 4.2 K and assuming validity of the Curie law, is only 1.3%. The magnetic susceptibility is described by the sum of two contributions; one is from the spin-Peierls state (χ_{SP}) and the other is a paramagnetic contribution (χ_{Curie}).

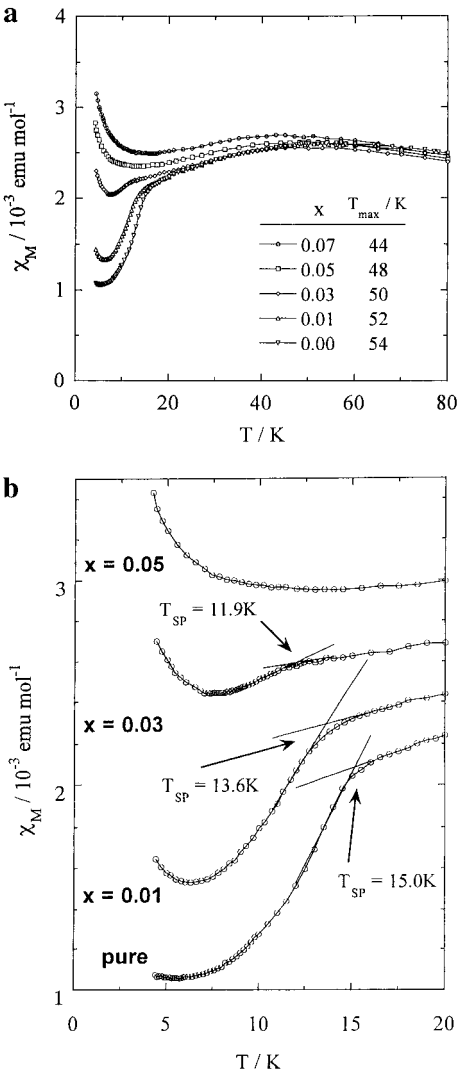

Figure 2. Magnetic susceptibility (χ_M) of mixed radical crystals, $(p\text{-CyDOV})_{1-x}(p\text{-BrDOV})_x$: (a) χ_M's of $x = 0$, 0.01, 0.03, 0.05, and 0.07 in the temperature range 4.2−80 K; (b) χ_M's of $x = 0$, 0.01, 0.03, and 0.05 in the temperature range 4.2−20 K. In (b), the vertical positions are shifted by 0.2×10^{-3} emu/radical mol. T_{SP}'s are defined as the temperature of the intersection of two lines along susceptibility curves above and below T_{SP}.[13]

$$\chi_M = C_{SP}\chi_{SP} + C_{Curie}\chi_{Curie} \quad (1)$$

where $C_{SP} = 0.987$ and $C_{Curie} = 0.013$ for the pure *p*-CyDOV crystal ($x = 0$), and χ_{Curie} is given by $\chi_{Curie} = N_o g^2 \mu_B^2 S(S + 1)/3k_B T$ with $S = {}^1/_2$.

The χ_M of the pure *p*-BrDOV crystal ($x = 1$) is shown in Figure 3 as a function of temperature. The χ_M of *p*-BrDOV shows a broad maximum at $T_{max} = 34.0 \pm 0.7$ K. A small increase in susceptibility below 7.1 K was observed, which will

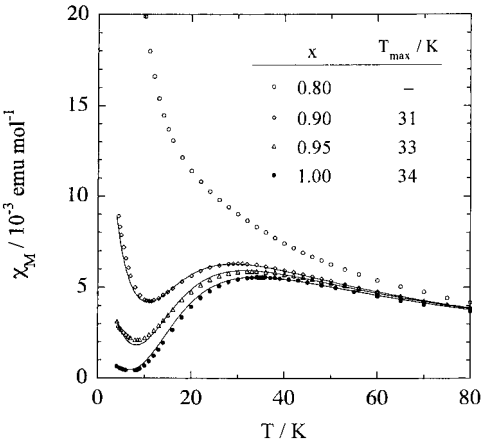

Figure 3. Magnetic susceptibility (χ_M) of mixed radical crystal, (p-CyDOV)$_{1-x}$(p-BrDOV)$_x$ (x = 0.80, 0.90, 0.95, and 1) in the temperature range 4.2−80 K.

be attributable to isolated monoradicals. The susceptibility of p-BrDOV can be well explained by the sum of the two contributions;

$$\chi_M = C_{Dimer}\chi_{Dimer} + C_{Curie}\chi_{Curie} \quad (2)$$

where the first and second terms represent the contributions from the dimer system (the singlet−triplet equilibrium model) and from the Curie impurity, respectively. χ_{Dimer} is given by $\chi_{Dimer} = (N_o g^2 \mu_B{}^2/k_B T)[1/(3 + e^{-2J/k_B T})]$. The solid curve ($x$ = 1) in Figure 3 is a theoretical curve with C_{Dimer} = 0.9928 and C_{Curie} = 0.0072 and $2J/k_B$ = −55 K.

Magnetic Susceptibilities of the Mixed Radical Crystals, (p-CyDOV)$_{1-x}$(p-BrDOV)$_x$ (x = 0−1). The magnetic susceptibilities of the mixed radical crystals, (p-CyDOV)$_{1-x}$(p-BrDOV)$_x$ (x = 0−1), were measured to study the effects of magnetic impurities on the SP transition and dimer states of p-CyDOV and p-BrDOV crystals, respectively. Figure 2 shows the temperature dependence of χ_M of the mixed radical crystals, (p-CyDOV)$_{1-x}$(p-BrDOV)$_x$ (x = 0−0.07), where χ_M is the magnetic susceptibility per 1 mol of p-CyDOV and p-BrDOV radicals as a total. By lowering the temperature from 300 K, the susceptibility of each mixed crystal increases gradually and shows a broad maximum at the temperature of T_{max}. The χ_M's above 60 K show only a weak x dependence. However, we can see that χ_M's below about 60 K drastically change with doping. The value of T_{max} decreases as the concentration (x) of p-BrDOV increases; T_{max}'s are 54 K for x = 0, 52 K for 0.01, 50 K for 0.03, 48 K for 0.05, and 44 K for 0.07. The SP transition indicated by a drop of χ_M near 12−15 K was observed in the samples with $x \le 0.03$ (Figure 2a,b). The values of T_{SP} defined as the onset temperature of the drop of the susceptibility are listed in Table 1. The x dependence of T_{SP} is shown in Figure 4. The value of $T_{SP}(x)/T_{SP}(0)$ linearly reduces up to $x \le 0.03$, which is expressed as $1 - 6.7x$. This means that the value of T_{SP} rapidly decreases by a small amount of p-BrDOV substitution. On the other hand, the χ_M's for x = 0.05 and 0.07 show no SP transition and monotonically increase as temperature is lowered below 13 K.

The x dependence of magnetic susceptibility (χ_M) of mixed radical crystals, (p-CyDOV)$_{1-x}$(p-BrDOV)$_x$ (x = 0.80−1), at a high concentration region of p-BrDOV is shown in Figure 3. The $\chi_M - T$ curves for x = 1, 0.95, 0.90, and 0.85 show a broad maximum at T_{max} = 34, 33, 31, and 29 K, respectively. At the low-temperature region, each susceptibility curve shows the existence of a Curie impurity, as observed for the pure p-BrDOV radical crystal (x = 1). For instance, in the case of the mixed radical crystal with x = 0.90, by subtracting the low-temperature Curie impurity curve (C_{Curie}) from the experimental one with T_{max} = 31 K, the corrected susceptibility with $T_{max}{}^{Corr}$ = 33 K (data are not shown) is obtained. This susceptibility can be well explained by a theoretical curve calculated for the singlet−triplet equilibrium model (χ_{Dimer}) with the value of $2J/k_B = -1.61T_{max}{}^{Corr} = -53$ K. The χ_M's of the mixed radical crystals with x = 0.95 and 0.85 are also well explained by eq 2, that is, the sum of the dimer term and the Curie impurity term. The theoretical curves (solid line) in Figure 3 show good agreement with the experimental data. The values of T_{max} and C_{Curie} obtained for these radical crystals are listed in Table 1. The $T_{max}{}^{Corr}$ values and $2J/k_B$ are also listed in Table 1. The value of T_{max} decreases and the Curie impurity (C_{Curie}) increases by decreasing the value of x. On the other hand, the $T_{max}{}^{Corr}$ values, that is, the intradimer exchange interactions ($2J/k_B$) observed, remain unchanged upon p-CyDOV substitution.

The dimer state in the p-BrDOV system survives even in the heavily doped sample with a magnetic impurity concentration of 15%. On the other hand, the SP state of p-CyDOV almost disappears in the lightly doped sample with an impurity concentration of 5%.

Powder X-ray Diffraction Patterns of the Mixed Radical Crystals, (p-CyDOV)$_{1-x}$(p-BrDOV)$_x$ (x = 0−1). Figure 5 shows the powder X-ray diffraction patterns of mixed radical crystals, (p-CyDOV)$_{1-x}$(p-BrDOV)$_x$ (x = 0, 0.07, 0.50, 0.85, and 1), in the range 2θ = 5−40° at room temperature. The X-ray diffraction pattern of the p-CyDOV radical crystal (x = 0) is quite different from that of the p-BrDOV crystal (x = 1). However, the diffraction patterns of mixed radical crystals with x = 0.01, 0.03, 0.05, 0.07, and 0.09 are quite similar to that of the pure p-CyDOV crystal (x = 0). The diffraction pattern due

TABLE 1: Magnetic Properties of the Mixed Radical Crystals (p-CyDOV)$_{1-x}$(p-BrDOV)$_x$ (x = 0−1)

x	T_{max} (K)	$T_{max}{}^{Corr}$ (K)	$2J/k_B$ (K)	T_{SP} (K)	C_{Curie}	C_{SP} ($T < T_{SP}$)	C_{1D-HAF} ($T < T_{SP}$)	C_{1D-HAF} ($T > T_{SP}$)
0	54	54	−84	15.0	0.013	0.987	0	0.987
0.01	52	54	−84	13.6	0.006	0.534	0.460	0.994
0.03	50	54	−84	11.9	0.008	0.153	0.840	0.992
0.05	48	53.3	−83.2		0.013		0.987	0.987
0.07	44	52.2	−81.4		0.016		0.984	0.984
0.09								
0.80						C_{Dimer}		
0.85	29	34	−55		0.096	0.904		
0.90	31	33	−53		0.10	0.90		
0.95	33	33	−53		0.034	0.966		
1	34	34	−55		0.0072	0.9928		

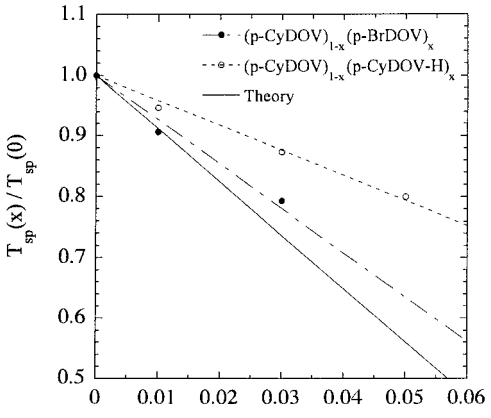

Figure 4. x dependence of spin-Peierls transition temperature (T_{SP}) of (a) mixed radical crystals, (p-CyDOV)$_{1-x}$(p-BrDOV)$_x$ (●), and (b) diluted radical crystals (p-CyDOV)$_{1-x}$(p-CyDOV−H)$_x$ (○).

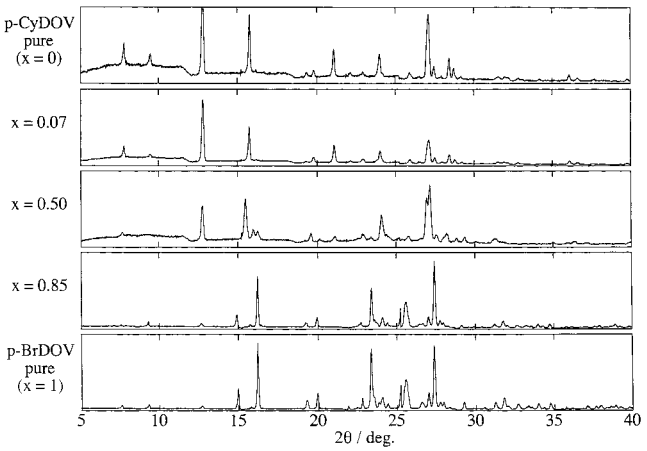

Figure 5. Powder X-ray diffraction patterns at room temperature for the mixed radical crystals, $(p\text{-CyDOV})_{1-x}(p\text{-BrDOV})_x$. Ranges $5° \leq 2\theta \leq 40°$.

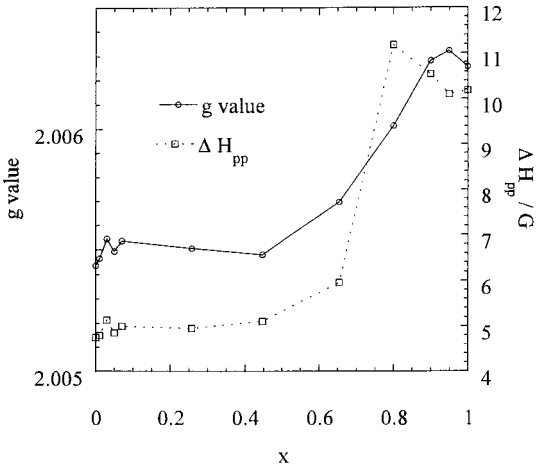

Figure 6. x dependence of the g value and the peak-to-peak line width (ΔH_{PP}) of mixed radical crystals, $(p\text{-CyDOV})_{1-x}(p\text{-BrDOV})_x$ ($x = 0-1$).

to the *p*-BrDOV crystal was not observed for the mixed radical crystals ($x = 0.01-0.09$). The result indicates that the *p*-BrDOV radical molecule homogeneously distributes in the AFM chains of the *p*-CyDOV in each sample, and the crystal structure of mixed radical crystals ($x = 0.01-0.09$) is almost the same as that of the pure *p*-CyDOV ($x = 0$) at room temperature.

Similarly, the X-ray diffraction patterns of mixed radical crystals ($x = 0.85$, 0.90, and 0.95) at the high concentration region of *p*-BrDOV are quite similar to that of the pure *p*-BrDOV crystal ($x = 1$), suggesting that the *p*-CyDOV molecule homogeneously distributes in the dimer system of the *p*-BrDOV in each sample and the crystal structure of the mixed crystals ($x = 0.85-0.95$) is almost the same as that of the pure *p*-BrDOV ($x = 0$) at room temperature. On the other hand, the X-ray diffraction pattern of the mixed radical crystal with $x = 0.50$ consists of the addition of those of *p*-CyDOV and *p*-BrDOV, although the contribution of the former is more remarkable than that of the latter, as shown in Figure 5.

ESR Spectra of the Mixed Radical Crystals, $(p\text{-CyDOV})_{1-x}$-$(p\text{-BrDOV})_x$ ($x = 0-1$). The ESR measurements were carried out in powder samples of the 12 kinds of mixed radical crystals, $(p\text{-CyDOV})_{1-x}(p\text{-BrDOV})_x$ ($x = 0-1$), at 25 °C. The notable x dependence of the ESR spectrum was observed. The ESR spectra of both the pure *p*-CyDOV and *p*-BrDOV radical crystals show an exchange-narrowed, Lorentz-type absorption located at $g = 2.0054$ and 2.0063 with a peak-to-peak line width (ΔH_{PP}) of 4.8 and 10.2 G, respectively. The x dependence of the g value and line width (ΔH_{PP}) is shown in Figure 6. At the region of $x = 0-0.45$, the line widths show a constant value of about 4.9 $\pm$ 0.2 G and increase rapidly at $x = 0.65$. Above $x = 0.80$ line widths show again a constant value of about 10.5 $\pm$ 0.7 G. The x dependence of the g value is similar to that of the line width, as shown in Figure 6. The result of ESR measurements also indicates that the *p*-BrDOV molecule homogeneously distributes in the 1D AFM chains of the *p*-CyDOV in each sample at the region of $x = 0-0.45$, and inversely, the *p*-CyDOV molecule homogeneously distributes in the dimer system of the *p*-BrDOV in the region $x = 0.80-1$.

Spin Density Distributions of the *p*-CyDOV and *p*-BrDOV Radical Molecules. The McLachlan spin densities (ρ_i)[24] of the *p*-CyDOV and *p*-BrDOV radicals were calculated by using the following MO parameters:[24] $\alpha_{N(1)} = \alpha + 1.2\beta$, $\alpha_{N(2)} = \alpha + 1.0\beta$, $\beta_{C-N} = 0.8\beta$, $\beta_{N-N} = 1.0\beta$ for the nitrogen atom of the verdazyl ring, $\alpha_O = \alpha + 2.0\beta$, $\beta_{C-O} = 1.4\beta$ for the oxygen atom of the carbonyl group, $\alpha_{CH_3} = \alpha + 2.0\beta$, $\beta_{N-CH_3} = 1.0\beta$ for the methyl group, $\alpha_{Br} = \alpha + 1.5\beta$, $\beta_{C-Br} = 0.3\beta$ for the bromine (Br) atom, and $\alpha_{N(15)} = \alpha + 0.5\beta$, $\beta_{N(15)-C(14)} = 1.2\beta$ for the nitrogen atom of the cyano group. The resonance integral $\beta_{C(3)-C(7)} = \beta \cos 12.3°$, where the choice of 12.3° was made on the basis of the results of the X-ray analysis of the 1,3,5-triphenyl-6-oxoverdazyl radical crystal.[3] The McLachlan MO parameter λ was given the standard value of 1.2. The spin densities (ρ_i) calculated with these parameters are given in Figure 1, indicating that the unpaired spin distributions of the *p*-CyDOV radical are very similar to those of the *p*-BrDOV radical.

Discussion

Doping Effect of Magnetic Impurities (*p*-BrDOV) on the Spin-Peierls Transition of the *p*-CyDOV Radical Crystal. In the present work, we measured the temperature dependence of the magnetic susceptibility (χ_M) of the 11 kinds of mixed radical crystals, $(p\text{-CyDOV})_{1-x}(p\text{-BrDOV})_x$ ($x = 0-1$).

To study the effects of magnetic impurities for the spin-Peierls (SP) transition of the *p*-CyDOV radical crystal, the *p*-BrDOV radical was chosen as the best dopant. First, *p*-BrDOV is expected to be substituted easily for *p*-CyDOV, because the molecular size, that is, the van der Waals radius of *p*-BrDOV, is thought to be similar to that of *p*-CyDOV, except for the difference of 2.5% in the lengths of long axes of the *p*-CyDOV (13.75 Å) and *p*-BrDOV (13.41 Å) radical molecules.[3] In fact, as shown in Figure 5, the X-ray diffraction patterns of the mixed radical crystals ($x = 0.01$, 0.03, 0.05, 0.07, and 0.09) are quite similar to that of the pure *p*-CyDOV crystal ($x = 0$). The result indicates that the *p*-BrDOV radical molecule homogeneously distributes in the quasi-1D AFM chains of the *p*-CyDOV in each sample, and the lattice constants are almost independent of x in this concentration range. Second, both *p*-CyDOV and *p*-BrDOV molecules are magnetic and have spin $S = {}^1/_2$. Third, we can expect that *p*-BrDOV has an electronic structure similar to that of *p*-CyDOV. In fact, the results of the McLachlan MO calculations indicate that the *p*-BrDOV molecule has an unpaired electron distribution very similar to that of *p*-CyDOV, as shown in Figure 1. Therefore, we can expect similar magnetic properties for the mixed radical crystals with $x = 0-0.09$.

In fact, in the region of $x = 0-0.09$, both the g value and line width show constant values of 2.0055 $\pm$ 0.0001 and 4.9 $\pm$ 0.2 G at 25 °C, respectively, as shown in Figure 6 and listed in Table 2. Similarly, the susceptibilities of the mixed radical crystals ($x = 0.01-0.07$) above 60 K show behaviors similar to each other, as shown in Figure 2. The result suggests that in this system the intermolecular exchange interaction ($2J_{Cy-Br}$)

TABLE 2: *g* Values and Line Widths (ΔH_{pp}) of the Mixed Radical Crystals (p-CyDOV)$_{1-x}$(p-BrDOV)$_x$ ($x = 0-1$)

x	g value	ΔH_{pp}/G
0	2.0054	4.8
0.01	2.0055	4.8
0.03	2.0055	5.1
0.05	2.0055	4.9
0.07	2.0055	5.0
0.26	2.0055	5.0
0.45	2.0055	5.1
0.65	2.0057	6.0
0.80	2.0060	11.2
0.90	2.0063	10.5
0.95	2.0063	10.1
1	2.0063	10.2

between the neighboring p-CyDOV and p-BrDOV radical molecules is almost identical with the $2J_{Cy-Cy}$ between the neighboring p-CyDOV molecules and the doping of magnetic impurity does not affect the propagation of spin correlations.

However, below 60 K, the χ_M's of mixed radical crystals show notable x dependence at the low concentration region of p-BrDOV ($0.01 \le x \le 0.07$), and the T_{SP} drastically changes with doping, as shown in Figure 2a,b. As described in a previous section, the value of T_{max} decreases as the concentration (x) of p-BrDOV increases. The SP transition indicated by a drop of χ_M near 12−15 K was observed in the samples with $x \le 0.03$. The χ_M's for $x = 0.05$ and 0.07 show no SP transition and monotonically increase as the temperature is lowered below 13 K. The increase of χ_M at low temperature indicates the existence of a Curie impurity, as also observed for the pure p-CyDOV radical crystal.

First, we tried to explain the susceptibilities for $x = 0.05$ and 0.07 by using the 1D Heisenberg antiferromagnetic (1D HAF) linear chain model with $T_{max} = 48$ and 44 K, respectively. However, the susceptibilities could not be explained by the above model; for instance, the theoretical values[23] of the susceptibility ($\chi_{max} = 0.142/T_{max} = 2.96 \times 10^{-3}$ and 3.23×10^{-3} emu/mol) at $T_{max} = 48$ and 44 K are 13 and 20% higher than the experimental values ($\chi_{max} = 2.62 \times 10^{-3}$ and 2.69×10^{-3} emu/mol) for $x = 0.05$ and 0.07, respectively. We found that the temperature dependence of χ_M can be simply described by the sum of the two contributions; one is from the 1D Heisenberg AFM linear chain system (χ_{1D-HAF}) with corrected T_{max}^{Corr} values and the other is a paramagnetic contribution (χ_{Curie}).

$$\chi_M = C_{1D-HAF}\chi_{1D-HAF} + C_{Curie}\chi_{Curie} \quad (3)$$

where $C_{1D-HAF} + C_{Curie} = 1$. The calculated results using eq 3 reproduce well the general features of the experimental data for $x = 0.05$ and 0.07, as shown by the solid curves in Figure 7. Similarly, the temperature dependence of the χ_M's for the mixed radical crystals with $x = 0.01$ and 0.03 above T_{SP} has been analyzed by using eq 3. The observed C_{1D-HAF}, T_{max}^{Corr}, $2J/k_B$, and C_{Curie} values are listed in Table 1. The intrachain exchange interactions ($2J/k_B$) obtained are similar to or slightly smaller than that for the pure p-CyDOV crystal. On the other hand, the χ_M's of the mixed radical crystals with $x = 0.01$ and 0.03 below T_{SP} cannot be explained only by the contributions of two terms, that is, eq 1 used for the pure p-CyDOV crystal or eq 3 used for the mixed crystal with $x = 0.05$ and 0.07. We assume that χ_M is described by three terms:

$$\chi_M = C_{SP}\chi_{SP} + C_{Curie}\chi_{Curie} + C_{1D-HAF}\chi_{1D-HAF} \quad (4)$$

where $C_{SP} + C_{Curie} + C_{1D-HAF} = 1$. χ_{SP} and χ_{1D-HAF} in eq 4 are the same as those in eqs 1 and 3, respectively, and χ_{SP} was

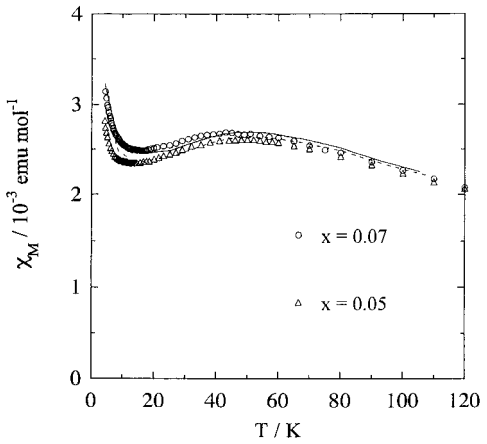

Figure 7. Magnetic susceptibility (χ_M) of mixed radical crystals, (p-CyDOV)$_{1-x}$(p-BrDOV)$_x$ ($x = 0.05$ and 0.07) in the temperature range 4.2−120 K. The χ_M's of the mixed radical crystals ($x = 0.05$ and 0.07) are well reproduced by eq 3 (solid and dotted lines).

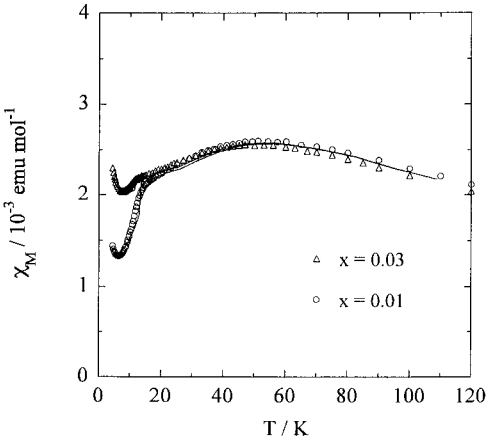

Figure 8. Magnetic susceptibility (χ_M) of mixed radical crystals, (p-CyDOV)$_{1-x}$(p-BrDOV)$_x$ ($x = 0.01$ and 0.03) in the temperature range 4.2−120 K. The χ_M's of the mixed radical crystals ($x = 0.01$ and 0.03) are well reproduced by eq 4 (solid line).

calculated from the χ_M's for the pure p-CyDOV ($x = 0$) below T_{SP} by using eq 1. As the χ_{1D-HAF} in eq 4, the susceptibility for the 1D Heisenberg AFM linear chain system with $2J/k_B = -84$ K was used, as listed in Table 1.[23]

As described above, contributions from the second term are estimated to be $C_{Curie} = 0.006$ for $x = 0.01$ and 0.008 for $x = 0.03$ from the susceptibility above T_{SP}. Contributions from the first (C_{SP} χ_{SP}) and third (C_{1D-HAF} χ_{1D-HAF}) terms have been tentatively estimated by comparing the experimental data with the calculated results using eq 4. The χ_M's of the mixed radical crystals ($x = 0.01$ and 0.03) are well reproduced by eq 4, as shown by the solid curves in Figure 8. The C_{SP} and C_{1D-HAF} values obtained are listed in Table 1.

Recently, the effects of magnetic (Mn^{2+} ($S = {}^5/_2$),[21] Ni^{2+} ($S = 1$)[21] and Co^{2+} ($S = {}^3/_2$),[25] and nonmagnetic (Zn^{2+} ($S = 0$)[19,20,26−28] and Mg^{2+} ($S = 0$)[29,30]) impurities have been studied for the SP transition of $CuGeO_3$ (Cu^{2+} ($S = {}^1/_2$)). Similar studies have been performed for the Si-doped $CuGeO_3$ ($CuGe_{1-x}Si_xO_3$).[21,28,31,32] The SP transition temperature ($T_{SP} = 14.2$ K) decreased rapidly by increasing the concentration (x) of impurities and disappeared at around $x = 0.01-0.04$ depending on the kinds of impurities. A detailed study of the effects of impurities on the SP system was performed for the $Cu_{1-x}Zn_xGeO_3$ system ($T_{SP} = 14.2$ K) by Hase et al.[19,20] and Oseroff et al.[21] The SP transition temperature (T_{SP}) linearly reduces, following the equation T_{SP}-

$(x)/T_{SP}(0) = 1 - 13.7x$, and the SP state collapses around $x = 0.03$. Further, they discovered an AFM phase transition in the samples with $0.02 \leq x \leq 0.08$ below 4.5 K.[20,21] It has been found that such an AFM transition takes place below 5 K not only in $Cu_{1-x}Zn_xGeO_3$[27,28] but also in $Cu_{1-x}M_xGeO_3$ (M = Mg,[30] Ni,[21] Mn[21]) and $CuGe_{1-x}Si_xO_3$[28,31,32] systems.

One of the most interesting phenomena observed in these doped $CuGeO_3$ systems is the coexistence of the long-range order of the lattice dimerization, which is intrinsic to the SP phase, and the AFM long-range order. The neutron scattering experiments were studied on Si-[31,32] and Zn-doped[27] $CuGeO_3$, and both a dimerization superlattice peak and an AFM peak were observed. Fukuyama et al.[33] theoretically explained the coexistence of the dimerization and the AFM long-range order in $CuGe_{1-x}Si_xO_3$ using a phase Hamiltonian. According to their theory, the coexistence of the dimerization and $\langle S^Z \rangle$ of spins on Cu^{2+} ions with spatially inhomogeneous distribution has been suggested. A recent μSR study[28] on Zn- and Si-doped $CuGeO_3$ indicated the spatial inhomogeneity of $\langle S^Z \rangle$ of spins on Cu^{2+} ions in AFM long-range order phase, which supports the theory of Fukuyama et al. Further, Masuda et al.[30] studied the temperature (T)−impurity concentration (x) phase diagram in $Cu_{1-x}Mg_xGeO_3$ in detail and found (i) the clear disappearance of T_{SP} at the critical impurity concentration (x_C) and the corresponding jump of T_N and (ii) the existence of different AFM long-range orders (dimerized-AFM and uniform-AFM long-range orders) with and without the lattice dimerization below and above x_C, respectively.

A similar effect of nonmagnetic impurity has been observed for the SP transition of the organic verdazyl radical crystal, *p*-CyDOV.[13,34] By the doping of the nonmagnetic reduced form (*p*-CyDOV−H) of *p*-CyDOV, the SP transition temperature decreased rapidly, following the equation $T_{SP}(x)/T_{SP}(0) = 1 - 4.2x$, and the SP transition disappeared at $x = 0.07$.

Ajiro et al.[29] reported that both the susceptibilities and the high-field magnetization curves ($H = 0-40$ T) of the inorganic spin-Peierls system ($Cu_{1-x}Mg_xGeO_3$, $x = 0.02$ and 0.04) including Mg^{2+} ion as a nonmagnetic impurity below T_{SP} can be explained by the three term contributions (eq 5), where the

$$\chi_M = C_{SP}\chi_{SP} + C_{Curie}\chi_{Curie} + C_{AFM}\chi_{AFM} \qquad (5)$$

third term represents the contribution from the AFM phase, as found for the inorganic SP system, $Cu_{1-x}Zn_xGeO_3$ ($0.02 \leq x \leq 0.08$), below the Neel temperature T_N. They have succeeded in estimating the contribution from each term in eq 5 from the results of the above measurements. The result also supports the coexistence of SP and AFM orderings in the $Cu_{1-x}Mg_xGeO_3$ system at low temperature.

In the present work, similar analyses have been performed for the mixed radical crystals, (p-CyDOV)$_{1-x}$(*p*-BrDOV)$_x$ ($x = 0-0.07$). The χ_M's of the mixed radical crystals with $x = 0.05$ and 0.07 ($x > x_C$) may be well explained by using eq 3, that is, by 1D Heisenberg linear chain model without the lattice dimerization, suggesting the appearance of uniform-AFM long-range order at lower temperature (T_N). On the other hand, the χ_M's of the mixed radical crystals with $x = 0.01$ and 0.03 ($x < x_C$) may be explained by using eq 4, as described above. The result suggests the coexistence of the SP and 1D HAF states, that is, the coexistence of micro SP and 1D HAF domains in the crystals below T_{SP}, differing from the coexistence of the dimerization and the dimerized- AFM long-range order in the doped $CuGeO_3$ systems. However, the details are not clear at present. At lower temperature below 4.2 K, AFM transition takes place, and χ_M's of the mixed radical crystals ($x = 0.01$ and 0.03) may be explained by the coexistence of the dimerization and the dimerized-AFM long-range order with spatial inhomogeneity in the ordered moment size, as observed for the doped $CuGeO_3$.

As described above, magnetic behavior of the mixed *p*-CyDOV radical crystals, (*p*-CyDOV)$_{1-x}$(*p*-BrDOV)$_x$ ($x = 0-0.07$) and the x dependence of the SP transition temperature (T_{SP}), that is, $T_{SP}(x)/T_{SP}(0) = 1 - 6.7x$, are similar to those of $Cu_{1-x}Zn_xGeO_3$ and (*p*-CyDOV)$_{1-x}$(*p*-CyDOV−H)$_x$ systems. We could not observe an AFM transition for the mixed *p*-CyDOV radical crystal at low temperatures. At low temperatures, we have to consider the effect from the interchain interaction (J'), which triggers the AFM transition at T_N. The mean field theory[35] gives the relation $k_BT_N \doteqdot 2S^2(|zJ'|J)^{1/2}$ (z, the number of neighboring chains). SP transition temperatures of *p*-CyDOV ($T_{SP} = 15.0$ K) and $CuGeO_3$ ($T_{SP} = 14.2$ K) are similar to each other. The χ_M's of *p*-CyDOV and $CuGeO_3$ show a broad maximum at 54 and 56 K above T_{SP}, respectively, suggesting similar AFM exchange interactions ($2J/k_B$) for these compounds. In fact, the susceptibility (χ_M) of *p*-CyDOV above T_{SP} can be well explained by the 1D Heisenberg linear chain model with an AFM exchange interaction of $2J/k_B = -T_{max}/0.641 = -84$ K between neighboring spins.[12,23] On the other hand, the χ_M of $CuGeO_3$ above T_{SP} cannot be explained by the simple 1D Heisenberg linear chain model with $2J/k_B = -88$K. The χ_M can be well described by the 1D Heisenberg model with competing AFM interactions, that is, first- and second-neighbor AFM exchange interaction of $2J_1/k_B = -150$ K and $2J_2/k_B = -34$ K, respectively.[36] Further, organic radical crystals generally show higher one-dimensionality than those of inorganic compounds, suggesting a smaller J' value for the former. Therefore, at a lower temperature, we can expect an AFM transition for the mixed *p*-CyDOV radical crystal. The measurement of heat capacity will be necessary, to ascertain the appearance of the AFM transition at low temperature.

The effects of doping on SP systems have been studied by Lu et al.,[37] using the unimolecular mean-field theory. It has been suggested that Zn doping results in a collapse of the spin gap and the existence of a gapless SP state for Zn concentration $x \geq 0.03$. They found that the $T_{SP}(x)$ is reduced by factor x following the eq 6, where $T_{SP}(0)$ is the SP transition temperature

$$T_{SP}(x)/T_{SP}(0) = 1 - 0.14x(2\sqrt{2|J|/k_BT_{SP}(0)})^2 \qquad (6)$$

without doping, and $2|J|$ is the intrachain exchange interaction according to Bonner and Fisher's work.[23] By substituting the values of $T_{SP}(0) = 15$ K and $2J/k = -84$ K into eq 6, we can obtain the relation $T_{SP}(x)/T_{SP}(0) = 1 - 8.8x$ for the (*p*-CyDOV)$_{1-x}$(*p*-BrDOV)$_x$ system. Reasonable agreement was observed for the system of (*p*-CyDOV)$_{1-x}$(*p*-BrDOV)$_x$, because the relation observed experimentally is $T_{SP}(x)/T_{SP}(0) = 1 - 6.7x$. On the other hand, the agreement between theory and experiment is not so good in the case of the (*p*-CyDOV)$_{1-x}$(*p*-CyDOV−H)$_x$ system; where the relations obtained theoretically and experimentally are $T_{SP}(x)/T_{SP}(0) = 1 - 8.8x$ and $T_{SP}(x)/T_{SP}(0) = 1 - 4.2x$, respectively. The difference between theoretical and experimental values in the diluted *p*-CyDOV radical system is not clear at present.

For the SP transition, a subtle balance is required between the magnetic energy gain due to the spin dimerization and the lattice energy loss due to distortion. It is likely that the SP transition will be suppressed locally by the impurity-induced lattice distortion, although the molecular size, that is, the van der Waals radius of *p*-BrDOV is thought to be similar to that of *p*-CyDOV, except for the difference of 2.5% in the lengths

of long axes of the *p*-CyDOV (13.75 Å) and *p*-BrDOV (13.41 Å) radical molecules. The SP compounds *p*-CyDOV and $CuGeO_3$ are molecular and ionic crystals, respectively. Generally, molecular crystals are thought to be "soft crystals", because molecules are connected by a weak van der Waals bond. Therefore, the lattice energy loss due to the doping of magnetic impurity in a molecular crystal will be smaller than that in an ionic crystal.

In the present mixed radical crystals $(p\text{-CyDOV})_{1-x}(p\text{-BrDOV})_x$ ($x = 0-0.07$), both *p*-CyDOV and *p*-BrDOV have spin $S = {}^1/_2$, and the intrachain exchange interaction ($2J_{Cy-Br}$) between the neighboring *p*-CyDOV and *p*-BrDOV radical molecules is similar to the $2J_{Cy-Cy}$ between the neighboring *p*-CyDOV molecules, as described above; that is, the substituted *p*-BrDOV molecules play a role as *p*-CyDOV ones in the mixed radical crystals with $x = 0-0.07$ above T_{SP}. Therefore, we can expect that the doping effect is not so remarkable in the present system. However, the T_{SP} decreased rapidly by increasing the concentration (x) of impurities and the SP transition disappeared in the lightly doped sample with an impurity concentration of 4−5%. The reason is not clear at present.

Doping Effect of Magnetic Impurities (*p*-CyDOV) on the Dimer State of the *p*-BrDOV Radical Crystal. The X-ray diffraction patterns of mixed radical crystals ($x = 0.85$, 0.90, and 0.95) at a high concentration region of *p*-BrDOV are quite similar to that of the pure *p*-BrDOV crystal ($x = 1$) (see Figure 5), indicating that the *p*-CyDOV molecules homogeneously distribute in the dimer system consisting of the *p*-BrDOV molecules in each sample, and the crystal structure of mixed crystals with $x = 0.85-0.95$ is almost the same as that of the pure *p*-BrDOV ($x = 1$) at room temperature. The unpaired spin distributions of the *p*-BrDOV radical are also very similar to those of the *p*-CyDOV radical, as shown in Figure 1. Therefore, we can expect similar magnetic properties for the samples with $x = 0.85-1$. In fact, the g value and line width of ESR spectra show constant values of 2.0063 ± 0.0002 and 10.3 ± 0.2 G at this region, respectively. Further, the intradimer exchange interaction $2J/k_B$ remains constant between $x = 0.85$ and 1, as listed in Table 1. The result suggests that the substituted *p*-CyDOV molecules play a role as *p*-BrDOV ones in the mixed radical crystals with $x = 0.85-1$, although the substitution induces the increase of the Curie impurity in the crystal.

Summary

In summary, we prepared the mixed radical crystals, $(p\text{-CyDOV})_{1-x}(p\text{-BrDOV})_x$ ($x = 0-1$), and measured the magnetic susceptibilities, ESR, and powder X-ray patterns to study the effects of magnetic impurities on the SP transition of *p*-CyDOV and the dimer cluster system of *p*-BrDOV. The SP transition temperature linearly reduces with increasing x and the SP state almost disappears even in the lightly doped sample with $x = 0.05$, although the 1D Heisenberg AFM exchange interaction ($2J/k_B$) remains constant between $x = 0$ and 0.07. On the other hand, the dimer state in *p*-BrDOV survives in the heavily doped sample with $x = 0.85$, and the intradimer exchange interaction $2J/k_B$ remains constant between $x = 0.85$ and 1. This work is the first report of the effects of magnetic impurities on the organic SP transition system.

Acknowledgment. This work was partly supported by the Grant-in-Aid for Scientific Research No. 08454225 from the Ministry of Education, Science, and Culture, Japan. We are very grateful to Prof. Yuji Soejima and Mr. Shuichiro Kuwajima of Kyushu University for their kind help in measuring the powder X-ray diffraction patterns of the mixed crystals by the STOE transmission X-ray diffractometer. We are also grateful to Mr. Naoki Wada for his kind help in the synthesis of the *p*-CyDOV radical crystal. We are very grateful to Prof. Yoshitami Ajiro for his helpful discussions.

References and Notes

(1) Proceedings of the Fifth International Conference on Molecular-Based Magnets. *Mol. Cryst. Liq. Cryst. Sec. A* **1997**, *305*, 1−586.
(2) Neugebauer, F. A.; Fisher, H.; Siegel, R. *Chem. Ber*. **1988**, *121*, 815.
(3) Neugebauer, F. A.; Fischer, H.; Krieger, C. *J. Chem. Soc., Perkin Trans. 2* **1993**, 535.
(4) Mukai, K.; Konishi, K.; Nedachi, K.; Takeda, K. *J. Magn. Magn. Mater*. **1995**, *140−144*, 1449.
(5) Mukai, K.; Nedachi, K.; Takiguchi, M.; Kobayashi, T.; Amaya, K. *Chem. Phys. Lett*. **1995**, *238*, 61.
(6) Mukai, K.; Konishi, K.; Nedachi, K.; Takeda, K. *J. Phys. Chem*. **1996**, *100*, 9658.
(7) Takeda, K.; Hamano, T.; Kawae, T.; Hidaka, M.; Takahashi, M.; Kawasaki, S.; Mukai, K. *J. Phys. Soc. Jpn*. **1995**, *64*, 2343.
(8) Kremer, R. K.; Kanellakopulos, B.; Bele, P.; Brunner, H.; Neugebauer, F. A. *Chem. Phys. Lett.* **1994**, *230*, 255.
(9) Mito, M.; Nakano, H.; Kawae, T.; Hitaka, M.; Takagi, S.; Deguchi, H.; Suzuki, K.; Mukai, K.; Takeda, K. *J. Phys. Soc. Jpn*. **1997**, *66*, 2147.
(10) Mukai, K.; Nuwa, M.; Morishita, T.; Muramatsu, T.; Kobayashi, T. C.; Amaya, K. *Chem. Phys. Lett*. **1997**, *272*, 501.
(11) Jamali, J. B.; Achiwa, N.; Mukai, K.; Suzuki, K.; Ajiro, Y.; Matsuda, K.; Iwamura, H. *J. Magn. Magn. Mater*. **1998**, *177−181*, 789.
(12) Mukai, K.; Wada, N.; Jamali, J. B.; Achiwa, N.; Narumi, Y.; Kindo, K.; Kobayashi, T.; Amaya, K. *Chem. Phys. Lett*. **1996**, *257*, 538.
(13) Jamali, J. B.; Wada, N.; Shimobe, Y.; Achiwa, N.; Kuwajima, S.; Soejima, Y.; Mukai, K. *Chem. Phys. Lett*. **1998**, *292*, 661.
(14) Hamamoto, T.; Narumi, Y.; Kindo, K.; Mukai, K. Shimobe, Y.; Kobayashi, T. C.; Muramatsu, T.; Amaya, K. *Physica B* **1998**, *246−247*, 36.
(15) Bray, J. W.; Hart, H. R., Jr.; Interrante, L. V.; Jacobs, I. S.; Kasper, J. S.; Watkins, G. D.; Wee, S. H.; Bonner, J. C. *Phys. Rev. Lett.* **1975**, *35*, 744.
(16) Jacobs, I. S.; Bray, J. W.; Hart, H. R., Jr.; Interrante, L. V.; Kasper, J. S.; Watkins, G. D.; Prober, D. E.; Bonner, J. C. *Phys. Rev*. **1976**, *B14*, 3036.
(17) Huizinga, S.; Kommandeur, J.; Sawatzky, G. A.; Thole, B. T.; Kopinga, K.; de Jonge, W. J. M.; Roos, J. *Phys. Rev*. **1979**, *B19*, 4723.
(18) Hase, M.; Terasaki, I.; Uchinokura, K. *Phys. Rev. Lett*. **1993**, *70*, 3651.
(19) Hase, M.; Terasaki, I.; Sasago, Y.; Uchinokura, K. *Phys. Rev. Lett*. **1993**, *71*, 4059.
(20) Hase, M.; Koide, N.; Manabe, K.; Sasago, Y.; Uchinokura, K.; Sawa, A. *Physica* **1995**, *B215*, 164.
(21) Oseroff, S, B.; Cheong, S.-W.; Aktas, B.; Hundley, M. F.; Fisk, Z.; Rupp, L. W. Jr. *Phys. Rev. Lett*. **1995**, *74*, 1450.
(22) McLachlan, A. D. *Mol. Phys*. **1960**, *3*, 233.
(23) Bonner, J. C.; Fisher, M. E. *Phys. Rev*. **1964**, *A135*, 640.
(24) Streitwieser, A., Jr. *Molecular Orbital Theory for Organic Chemists*; John Wiley & Sons: New York, London, 1961, 135.
(25) Elizabeth, S.; Babu, P. K.; Bhat, H. L. *Solid State Commun*. **1998**, *106*, 149.
(26) Hase, M.; Sasago, Y.; Terasaki, I.; Uchinokura, K.; Kido, G.; Hamamoto, T. *J. Phys. Soc. Jpn.* **1996**, *65*, 273.
(27) Martin, M. C.; Hase, M.; Hirota, K.; Shirane, G.; Sasago, Y.; Koide, N.; Uchinokura, K. *Phys. Rev.* **1997**, *B56*, 3173.
(28) Kojima, K. M.; Fudamoto, Y.; Larkin, M.; Luke, G. M.; Merrin, J.; Nachumi, B.; Uemura, Y. J.; Hase, M.; Sasago, Y.; Uchinokura, K.; Ajiro, Y.; Revcolevschi, A.; Renard, J.-P. *Phys. Rev. Lett*. **1997**, *79*, 503.
(29) Ajiro, Y.; Asano, T.; Masui, F.; Mekata, M.; Aruga-Katori, H.; Goto, T.; Kikuchi, H. *Phys. Rev. B* **1995**, *51*, 9399.
(30) Masuda, Y.; Fujioka, A.; Uchiyama, Y.; Tsukada, I.; Uchinokura, K. *Phys. Rev. Lett*. **1998**, *80*, 4566.
(31) Regnault, L. P.; Renard, J. P.; Dhalenne, G.; Revcolevschi, A. *Europhys. Lett*. **1995**, *32*, 579.
(32) Renard, J. P.; Dang, K. Le; Veillet, P.; Dhalenne, G.; Revcolevschi, A.; Regnault, L. P. *Europhys. Lett*. **1995**, *30*, 475.
(33) Fukuyama, H.; Tanimoto, T.; Saito, M. *J. Phys. Soc. Jpn*. **1996**, *65*, 1182.
(34) Mukai, K.; Wada, N.; Jamali, J. B.; Achiwa, N.; Narumi, Y.; Kindo, K.; Kobayashi, T.; Amaya, K. *Mol. Cryst. Liq. Cryst.* **1997**, *305*, 499.
(35) Steiner, M.; Villain, J.; Windsor, C. G. *Adv. Phys*. **1976**, *25*, 87.
(36) Castilla, G.; Chakravarty, S.; Emery, V. J. *Phys. Rev. Lett*. **1995**, *75*, 1823.
(37) Lu, Z. Y.; Su, Z. B.; Yu, L. *Phys. Rev. Lett*. **1994**, *72*, 1276.